



Buckling of FRP Long Tubes Lined with Steel Pipe under External Pressure

Hayder A. Rasheed¹

Abstract

The elastic stability of rings/long FRP tubes under external fluid pressure is very well studied. The formula for critical hydrostatic buckling pressure of thin cylindrical shells has been derived in closed form. These composite shells have attracted a lot of attention to use in deep water offshore drilling due to the weight advantage. A new design is proposed here using an FRP tube lined with a steel pipe. The metal shell also acts as a permanent mandrel for the filament winding process of the outer laminated composite shell. A generalized closed form analytical formula for the buckling of thin FRP-Steel multi-angle laminated long cylinders is developed. Standard energy based formulation is used to express the kinematics and equilibrium equations of the shells. Effective moduli are obtained to introduce the constitutive equations of thin shells. These equations are directly integrated to produce effective axial, coupling and flexural rigidities. Comparisons are made with some existing results.

1. Introduction

The stability analysis of tubular components has attracted a lot of attention since the mid 1800's. This is attributed to their wide range of applications in aerospace, automotive, marine, civil and offshore structures. In those applications, cylindrical shells are subjected to a combination of loads that result in compromising their structural integrity. One of such important loads for under water applications is external hydrostatic pressure. Traditionally, the majority of pipelines and tubes were constructed of steel and other metals. Nevertheless, the use of fiber-reinforced polymers has rapidly increased since the 1950's due to their high stiffness and strength to weight ratio as well as their fatigue and corrosion resistance.

Filament wound laminated composite cylindrical shells were proposed to use for offshore oil drilling and production to significantly reduce the weight of risers and tethers and make it possible to push the envelope further by exploring deeper water applications (Sparks 1986). However, metal pipe pieces are typically connected by attaching flanges to the end of each tube and bolting the flanges together as the tubes are lowered in place, see Fig. 1. Using the same splicing technique for composite tubes introduces high stress concentration hot spots at the junction of the tube and the flange requiring a change in the design. It is also very hard to manufacture the flange ends with the tubes in one piece through the filament winding process. To overcome this difficulty while maintaining this efficient splicing technique, the author is

¹ Professor, Kansas State University, <hayder@ksu.edu>

proposing the use of hybrid steel-composite tubes. With this design, a steel shell is used as a mandrel to filament wind the composite shell wall on top. The metal inner shell helps cure the outer composite shell faster since metals conduct heat very efficiently. The hybrid shell produced is more cost effective if glass fibers are used instead of carbon fibers. Unlike carbon fiber-reinforced polymer, the coefficient of thermal expansion of the steel and glass fiber-reinforced polymer is very close, thus avoiding the development of extra thermal stresses. Moreover, carbon FRP is conductive promoting corrosion while glass FRP is electricity inert offering better control of corrosion. Accordingly, the hybrid construction suggested here is a combination of steel and glass FRP.

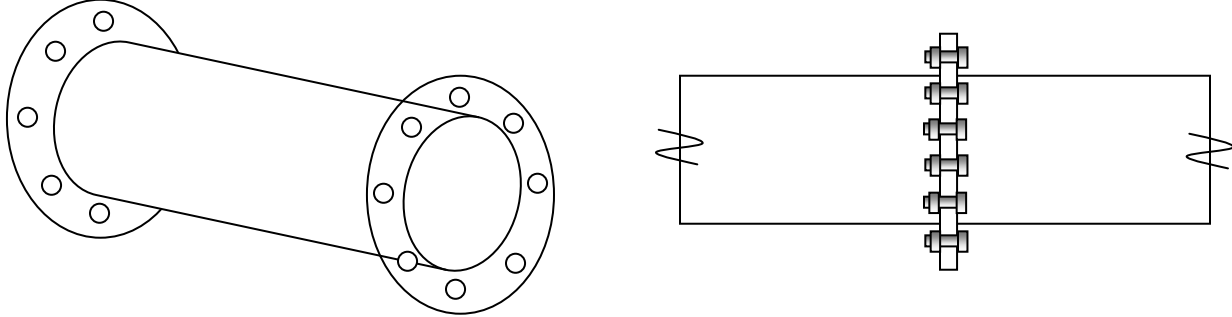


Figure 1: Typical steel tube splicing for offshore drilling applications.

Bresse (1866) was the first to calculate the buckling pressure of a thin elastic isotropic ring under external hydrostatic pressure. Bryan (1888) modified the buckling pressure formula for a long cylinder after few years. Timoshenko (1933) examined the response of elastic isotropic rings having out of roundness imperfection.

$$\begin{aligned}
 p_{cr} &= \frac{3Et^3}{12R^3} \quad (\text{rings}) \\
 p_{cr} &= \frac{3E}{(1-\nu^2)} \frac{t^3}{12R^3} \quad (\text{long cylinders})
 \end{aligned} \tag{1}$$

where E is the isotropic modulus of elasticity, ν is the isotropic Poisson's ratio, t is the ring thickness and R is the mean radius.

Ambartsumyan (1961) modified the above formula to account for the critical buckling pressure of homogeneous orthotropic long cylinders, as follows:

$$p_{cr} = \frac{3E_2}{(1-\nu_{12}\nu_{21})} \frac{t^3}{12R^3} \tag{2}$$

where E_2 is the hoop modulus, ν_{12} is the Poisson ratio for axial load and $\nu_{21} = \nu_{12}E_2/E_1$. Rasheed and Yousif (2001) developed a closed form generalized analytical formula for the critical buckling under external fluid pressure of thin laminated rings and long cylinders having any composite orthotropic lay-up with the stiffness coupling terms included.

$$p_{cr} = 3 \left(\frac{1 - \left(\frac{\psi^2}{\alpha} \right)}{1 + \alpha + 2\psi} \right) \frac{D_{orth}}{R^3} = 3 \left(\frac{A_{orth}D_{orth} - B_{orth}^2}{A_{orth}R^3 + 2B_{orth}R^2 + D_{orth}R} \right) \tag{3}$$

It is obvious that the above equation reduces to that of equations (1) and (2) for thin isotropic or homogeneous orthotropic rings/long cylinders respectively, since $B_{orth} = \psi = 0$ and $\alpha \ll 1$ in such cases. Rasheed and Yousif (2005) extended their critical buckling pressure formula to thin laminated rings and long cylinders having any composite anisotropic lay-up with the stiffness coupling terms included.

$$p_{cr} = 3 \left(\frac{1 - \left(\frac{\psi^2}{\alpha} \right)}{1 + \alpha + 2\psi} \right) \frac{D_{ani}}{R^3} = 3 \left(\frac{A_{ani} D_{ani} - B_{ani}^2}{A_{ani} R^3 + 2B_{ani} R^2 + D_{ani} R} \right) \quad (4)$$

The present work is intended to develop closed form analytical expressions for the effective axial, coupling and flexural hoop stiffness of the hybrid steel-FRP design proposed here in. A similar critical buckling pressure formula of thin long cylinders having the stiffness coupling terms included is arrived at. This formula is used to assess some new experiments of composite construction with aluminum liner.

2. Analytical Formulation

Multi-angle laminated composite filament wound around a steel layer is considered in this formulation. However, to constrain the tube to orthotropic behavior, angle plies with $(\pm\alpha^\circ)$ are merged into one layer. This restricts the applicability of the present formulation to lay-ups with adjacent $(+\alpha^\circ)$ and $(-\alpha^\circ)$ plies. Nevertheless, this type of stacking sequence is widely used in filament wound cylinders since this manufacturing process inherently dictates adjacent $(\pm\alpha^\circ)$ layers.

Kinematics:

The kinematic relations follow the same expressions derived for thin isotropic rings (Brush and Almroth 1975). Figure 2 shows the Cartesian (X_2, X_3) and the polar (r, θ) coordinate systems used. For the intermediate class of deformations assumed, the hoop strain and circumferential line rotation are small. This results in the following displacement and strain-displacement relationships:

$$u^* = u ; \quad v^* = v + (r - R)\beta$$

$$\beta^* = \frac{v^* - u^{*'}}{r} = \beta = \frac{v - u'}{R} \quad (5)$$

where u^*, v^*, β^* are the radial, tangential displacements and rotation of a through-the-thickness circumferential line element (Figure 2), u, v, β are the corresponding displacement components of the mid-surface line. The hoop strains are accordingly expressed by:

$$\varepsilon_\theta = \frac{u + v'}{R} + \frac{\beta^2}{2}$$

$$\varepsilon_\theta^* = \frac{u + v'}{R} + \frac{\beta^2}{2} + \frac{(r - R)\beta'}{R} = \varepsilon_\theta + z\kappa_\theta \quad (6)$$

where $\varepsilon_\theta, \varepsilon_\theta^*$ are the hoop strains along the mid-surface and any other parallel surface, respectively, $\kappa_\theta = \beta'/R$ is the circumferential curvature of mid-surface. The same linear strain distribution is considered for the axial and shearing strains in thin shells for the sake of the closed form solution.

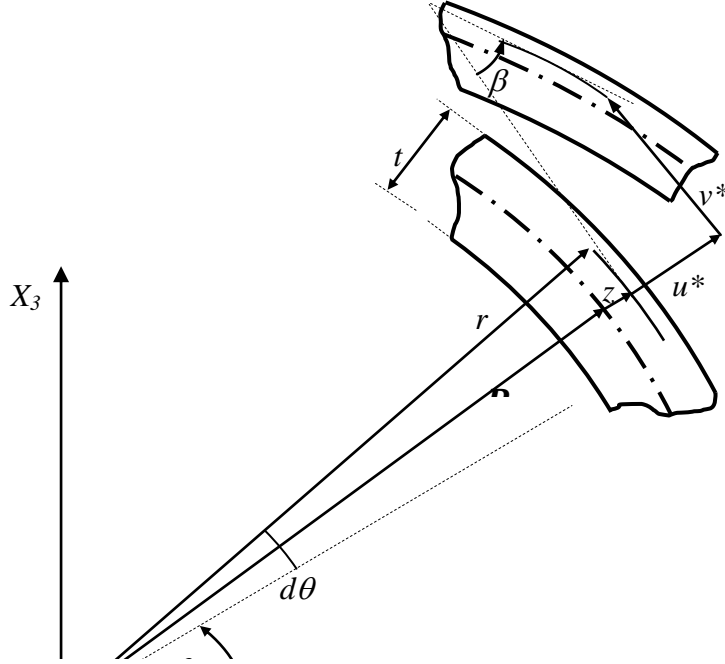


Fig.2 The shell in-plane geometry and deformation components

Figure.2 The shell in-plane geometry and deformation components

Constitutive Equations:

Transforming the material principle directions of every layer into the shell principle directions, the in-plane ply stress-strain relationship becomes:

$$\begin{Bmatrix} \sigma_x^* \\ \sigma_\theta^* \\ \tau_{x\theta}^* \end{Bmatrix} = \begin{bmatrix} \bar{Q}_{11} & \bar{Q}_{12} & \bar{Q}_{16} \\ \bar{Q}_{12} & \bar{Q}_{22} & \bar{Q}_{26} \\ \bar{Q}_{16} & \bar{Q}_{26} & \bar{Q}_{66} \end{bmatrix} \begin{Bmatrix} \varepsilon_x^* \\ \varepsilon_\theta^* \\ \gamma_{x\theta}^* \end{Bmatrix} \quad (7)$$

where \bar{Q}_{ij} are explicitly defined in composite textbooks in terms of the ply orthotropic material properties and the fiber inclination angle α with respect to the ring axis (Jones 1975). The assumption of orthotropic shell response dictates that adjacent $(\mp\alpha^\circ)$ layers are merged together. This causes (\bar{Q}_{16}) and (\bar{Q}_{26}) coefficients of equation (7) to vanish and the rest of the coefficients to equal the average value from the $(+\alpha^\circ)$ and $(-\alpha^\circ)$ plies. Reflecting this simplification and substituting equation (6) into (7):

$$\begin{Bmatrix} \sigma_x^* \\ \sigma_\theta^* \\ \tau_{x\theta}^* \end{Bmatrix} = \begin{bmatrix} \bar{Q}_{11} & \bar{Q}_{12} & 0 \\ \bar{Q}_{12} & \bar{Q}_{22} & 0 \\ 0 & 0 & \bar{Q}_{66} \end{bmatrix} \begin{Bmatrix} \varepsilon_x^* \\ \varepsilon_\theta^* \\ \gamma_{x\theta}^* \end{Bmatrix} = \begin{bmatrix} \bar{Q}_{11} & \bar{Q}_{12} & 0 \\ \bar{Q}_{12} & \bar{Q}_{22} & 0 \\ 0 & 0 & \bar{Q}_{66} \end{bmatrix} \begin{Bmatrix} \varepsilon_x + z\kappa_x \\ \varepsilon_\theta + z\kappa_\theta \\ \gamma_{x\theta} + z\kappa_{x\theta} \end{Bmatrix} \quad (8)$$

Due to the special displacement boundary conditions associated with the long cylinder problem, the above equation is possible to reduce to yield effective hoop local modulus.

$$\sigma_\theta^* = \bar{Q}_{22}(\varepsilon_\theta + z\kappa_\theta) \quad (9)$$

In the case of a steel layer, the hoop effective modulus is simply defined as:

$$\bar{Q}_{22} = \frac{E}{1-\nu^2} \quad (10)$$

In the case of a hoop orthotropic layer, the hoop effective modulus eventually reduces to:

$$\bar{Q}_{22} = \frac{E_1}{1-\nu_{12}\nu_{21}} \quad (11)$$

Similarly, in the case of a cross-ply layer, the hoop effective modulus reduces to:

$$\bar{Q}_{22} = \frac{1}{2} \left(\frac{E_1}{1-\nu_{12}\nu_{21}} + \frac{E_2}{1-\nu_{12}\nu_{21}} \right) \quad (12)$$

Also, in the case of an angle-ply layer, the hoop effective modulus is expanded as:

$$\bar{Q}_{22} = \frac{E_1}{1-\nu_{12}\nu_{21}} \sin^4 \alpha + 2 \left(\frac{\nu_{12}E_2}{1-\nu_{12}\nu_{21}} + 2G_{12} \right) \sin^2 \alpha \cos^2 \alpha + \frac{E_2}{1-\nu_{12}\nu_{21}} \cos^4 \alpha \quad (13)$$

Non-Linear Equilibrium Equations for External Fluid Pressure:

It can be easily shown that the strain energy stored in the orthotropic long cylinder is a function of the hoop stresses and strains only, since the axial displacements vanish:

$$U = \frac{1}{2} \int_V \sigma_\theta^* \varepsilon_\theta^* dV = \frac{1}{2} \int_{\theta} \int_{Area} \sigma_\theta^* \varepsilon_\theta^* dA r d\theta = \frac{R}{2} \int_{\theta} \int_{Area} \sigma_\theta^* (\varepsilon_\theta + z\kappa_\theta) dA \left(1 + \frac{z}{R}\right) d\theta \quad (14)$$

Knowing that ($dA = dz$) for a unit length of the cylinder in the axial direction and using equations (9), equation (14) becomes:

$$U = \frac{R}{2} \int_{\theta=-1/2}^{1/2} \bar{Q}_{22} (\varepsilon_\theta + z\kappa_\theta)^2 dz d\theta = \frac{R}{2} \left\{ \left[A_{eff} \int_{\theta=0}^{2\pi} \varepsilon_\theta^2 d\theta \right] + \left[2B_{eff} \int_{\theta=0}^{2\pi} \kappa_\theta \varepsilon_\theta d\theta \right] + \left[D_{eff} \int_{\theta=0}^{2\pi} \kappa_\theta^2 d\theta \right] \right\} \quad (15)$$

$$\text{where } A_{eff} = \sum_{k=1}^N \bar{Q}_{22k} t_k, \quad B_{eff} = \sum_{k=1}^N \bar{Q}_{22k} t_k \bar{z}_k, \quad D_{eff} = \sum_{k=1}^N \bar{Q}_{22k} t_k \left(\bar{z}_k^2 + \frac{t_k^2}{12} \right), \quad t_k = z_k - z_{k-1},$$

$$\bar{z}_k = \frac{z_k + z_{k-1}}{2}, \quad \text{and } N \text{ is the number of different layers in the stacking sequence.}$$

The potential of external fluid pressure loading is:

$$W = -p (V - V_0) = -p (A - A_0) \quad (16)$$

where (p) is the external pressure, ($A_0 = \pi R^2$) is the initial cross sectional area of the outer surface, (A) is the corresponding area in the deformed configuration. Writing (A) in terms of the displacement components and manipulating [8]:

$$W = \frac{-P}{2} \int_{\theta=0}^{2\pi} (2Ru + u^2 + v^2 + uv' - vu') d\theta \quad (17)$$

Defining the potential energy as $\Pi = U - W$, taking ($\delta\Pi = 0$), performing integration by parts, manipulating and considering arbitrary virtual displacements ($\delta u, \delta v$), the nonlinear equilibrium equations appear to be similar to those of isotropic rings:

$$\begin{aligned} -N_\theta' R + N_\theta \beta R - M_\theta' + pR^2 \beta &= 0 \\ M_\theta'' - N_\theta R - (N_\theta \beta)' R - p(u + v')R &= pR^2 \end{aligned} \quad (18)$$

Pre-buckling Solution:

The pre-buckling solution is obtained by substituting $u = u_o, v = 0, \beta = 0$, equations (6), $N_\theta = A_{eff} \varepsilon_\theta + B_{eff} \kappa_\theta$ and $M_\theta = B_{eff} \varepsilon_\theta + D_{eff} \kappa_\theta$ into equations (18). The first one is trivially satisfied and the second one gives:

$$\frac{u_o}{R} + \frac{p}{A_{eff}} u_o = -\frac{pR}{A_{eff}} \quad (19)$$

The second term above is negligible compared to that on the right hand side, yielding:

$$\frac{u_o}{R} = -\frac{pR}{A_{eff}} \quad (20)$$

Bifurcation Solution:

Substituting equations (6) and $N_\theta = A_{eff} \varepsilon_\theta + B_{eff} \kappa_\theta$ and $M_\theta = B_{eff} \varepsilon_\theta + D_{eff} \kappa_\theta$ into (18), perturbing the displacements u and v ($u \rightarrow u_0 + u_1, v \rightarrow v_1$) and linearizing:

$$\begin{aligned} \left(\frac{u_1' + v_1''}{R} \right) + \frac{B_{eff}}{A_{eff} R^2} (u_1' - u_1''' + 2v_1'') + \frac{D_{eff}}{A_{eff} R^3} (v_1'' - u_1''') &= 0 \\ \left(\frac{u_1 + v_1'}{R} \right) + \frac{B_{eff}}{A_{eff} R} \left[\left(\frac{-u_1' - v_1''}{R} \right)' + \beta_1' \right] - \frac{D_{eff}}{A_{eff} R^2} \beta_1''' + pR \left(\frac{u_1 + u_1''}{A_{eff} R} \right) &= 0 \end{aligned} \quad (21)$$

Note that the above equations differ from those of isotropic rings only by their additional coupling terms. For circular rings, u_1, u_1', v_1 and v_1' must be periodic, (u) is symmetric and (v) is anti-symmetric with respect to (X_3) axis [8], Fig. 2:

$$u_1 = c_2 \cos n\theta \quad \text{and} \quad v_1 = c_1 \sin n\theta \quad (22)$$

Assuming $\alpha = \frac{D_{eff}}{A_{eff}R^2}$; $\psi = \frac{B_{eff}}{A_{eff}R}$; $\gamma = \frac{pR}{A_{eff}}$ and substituting equation (22) into equations (21) and solving the eigenvalue system above for (γ):

$$\gamma = (n^2 - 1) \left(\frac{\alpha - \psi^2}{1 + \alpha + 2\psi} \right) \quad (23)$$

Equation (23) yields the critical buckling pressure, which may simply be expressed as:

$$p_{cr} = 3 \left(\frac{1 - \left(\frac{\psi^2}{\alpha} \right)}{1 + \alpha + 2\psi} \right) \frac{D_{eff}}{R^3} = 3 \left(\frac{A_{eff}D_{eff} - B_{eff}^2}{A_{eff}R^3 + 2B_{eff}R^2 + D_{eff}R} \right) \quad (24)$$

Effective Moduli:

Closed form expressions of the effective axial, coupling and flexural stiffness may be written for special cases of stacking sequence. For example, if the lay-up is composed of steel-hoop composite, the stiffness coefficients are written as:

$$\begin{aligned} A_{eff} &= \frac{Et_{steel}}{1-\nu^2} + \frac{E_1 t_{FRP}}{1-\nu_{12}\nu_{21}} \\ B_{eff} &= \frac{1}{2} \left(\frac{Et_{steel}}{1-\nu^2} (t_{steel} - t) + \frac{E_1 t_{FRP}}{1-\nu_{12}\nu_{21}} (t - t_{FRP}) \right) \\ D_{eff} &= \frac{1}{4} \left(\frac{Et_{steel}}{1-\nu^2} (t^2 - 2tt_{steel} + \frac{4}{3}t_{steel}^2) + \frac{E_1 t_{FRP}}{1-\nu_{12}\nu_{21}} (t^2 - 2tt_{FRP} + \frac{4}{3}t_{FRP}^2) \right) \end{aligned} \quad (25)$$

Also, if the lay-up is composed of steel/cross-ply composite, the stiffness coefficients are:

$$\begin{aligned} A_{eff} &= \frac{Et_{steel}}{1-\nu^2} + \bar{Q}_{FRP} t_{FRP} \\ B_{eff} &= \frac{1}{2} \left(\frac{Et_{steel}}{1-\nu^2} (t_{steel} - t) + \bar{Q}_{FRP} t_{FRP} (t - t_{FRP}) \right) \\ D_{eff} &= \frac{1}{4} \left(\frac{Et_{steel}}{1-\nu^2} (t^2 - 2tt_{steel} + \frac{4}{3}t_{steel}^2) + \bar{Q}_{FRP} t_{FRP} (t^2 - 2tt_{FRP} + \frac{4}{3}t_{FRP}^2) \right) \end{aligned} \quad (26)$$

Also, if the lay-up is composed of steel/angle-ply composite, the stiffness coefficients are:

$$\begin{aligned} A_{eff} &= \frac{Et_{steel}}{1-\nu^2} + \bar{Q}_{FRP} t_{FRP} \\ B_{eff} &= \frac{1}{2} \left(\frac{Et_{steel}}{1-\nu^2} (t_{steel} - t) + \bar{Q}_{FRP} t_{FRP} (t - t_{FRP}) \right) \\ D_{eff} &= \frac{1}{4} \left(\frac{Et_{steel}}{1-\nu^2} (t^2 - 2tt_{steel} + \frac{4}{3}t_{steel}^2) + \bar{Q}_{FRP} t_{FRP} (t^2 - 2tt_{FRP} + \frac{4}{3}t_{FRP}^2) \right) \end{aligned} \quad (27)$$

3. Applications

Sumana et al. (2015) have designed, built, tested and analyzed several composite tubes filament wound on top of an aluminum liner and subjected to external fluid pressure. The material properties of the aluminum and S-glass FRP are given in Table 1, as reported by Sumana et al. (2015). The aluminum pipe has an inner diameter of 80 mm, a wall thickness of 1 mm and a total length of 800 mm. The FRP was filament wound permanently on top of the aluminum liner using alternating cross-ply and angle-ply layers with a total thickness of 1 mm, 2 mm and 3 mm, respectively. The different layups implemented by Sumana et al. which are applicable to this paper are 0/90, $\overline{\overline{45}}$ and $\overline{\overline{55}}$. However, the sections at the two ends of the tube were fixed against deformation inside the pressure chamber (Sumana et al. 2015). On the other hand, the tube in the present analysis is assumed to be in a state of plane strain with all sections along its length deforming equally. If the tested tubes are long enough to have the tube mid-section not affected by its ends, the present solution would match the experimental one. However, if the tube ends affect the deformability of the middle section, then the present solution represents a lower bound solution to the test results. By examining the results obtained from the experiments compared to those generated by the present formula, it is evident that the AL-0/90 and the AL- $\overline{\overline{45}}$ tube specimens have the present solution represent a lower bound pressure to the experimental buckling pressure. This is attributed to the stiffening effect of the tube ends and the axial compression induced by the end capping pressure. On the other hand, the AL- $\overline{\overline{55}}$ tube specimen with 1 mm FRP still result in the same lower bound solution while the tube specimens with 2mm and 3 mm FRP show the opposite results. This may be attributed to the specific angle of 55 that has unequal effective hoop and axial moduli compared to the angle of 45 and 0/90 which has equal effective hoop and axial moduli in both cases. Overall, the present results have reasonable agreement to the experimental results despite the difference in the boundary conditions of the present analytical solution and the experimental results.

Table 1. Material Properties of Sumana et al. Tubes

Tube Material	E_{11}	E_{22}	G_{12}	ν_{12}
S Glass FRP	53.48 GPa	17.7 GPa	5.83 GPa	0.278
Aluminum 6061-T6	70 GPa	70 GPa	26.32 GPa	0.33

Table 2. External Buckling Pressure Comparison between Experiments and Present Solution

Tube Layup	Exp. P_{cr}	Present P_{cr}	t_{FRP}
AL-0/90	2.1268 MPa	1.5160 MPa	1 mm
AL-0/90	6.6555 MPa	4.9350 MPa	2 mm
AL-0/90	13.9949 MPa	11.1720 MPa	3 mm
AL- $\overline{\overline{45}}$	1.6939 MPa	1.2620 MPa	1 mm
AL- $\overline{\overline{45}}$	5.3597 MPa	4.0920 MPa	2 mm
AL- $\overline{\overline{45}}$	11.9832 MPa	9.3130 MPa	3 mm
AL- $\overline{\overline{55}}$	1.6140 MPa	1.4560 MPa	1 mm
AL- $\overline{\overline{55}}$	4.2720 MPa	4.7400 MPa	2 mm
AL- $\overline{\overline{55}}$	10.6018 MPa	10.7400 MPa	3 mm

4. Conclusions

A generalized buckling formula is developed for laminated orthotropic long cylinders made of glass fiber reinforced polymer lined with a metal pipe under external fluid pressure. The equation is expressed in terms of effective axial, coupling and flexural stiffness in the hoop direction, which are determined in closed form furnishing simple design calculations. The formula accounts for the effects of the axial and flexural modulus independently as well as the contribution of the ply coupling terms. The present formula is benchmarked against experimental results in the literature on the simpler cases of orthotropic laminated long cylinders.

Sumana et al. (2015) have designed, fabricated and tested nine composite tubes lined with identical aluminum pipes to study their buckling under external pressure. The buckling pressure formula is generally found to yield a lower bound solution of these tubes compared to the experiments due to the end boundary conditions of the tubes inside the pressure chamber. The only exception was the case of AL-~~T~~55 tubes with thicker FRP in which unequal effective moduli are experienced in the hoop vs. the axial directions. Overall, the results of the present formula are generally close to those of the experiments on the conservative side. This should encourage the engineers to use this solution in actual designs.

References

- Ambartsumyan, S. A., (1961) "Theory of Anisotropic Shells," NASA Technical Translation N64-22801-N64-22808.
- Bresse, M. (1866) "Cours de Mechanique Appliquée," 2nd Edition, Paris, France.
- Brush, D. O. and Almroth, B. O., (1975) "Buckling of Bars, Plates and Shells," McGraw Hill Inc., USA, 378 p.
- Bryan, G. H., (1888) Proceedings, Cambridge Philosophical Society, 6, Cambridge, UK.
- Jones, R. M., (1975) "Mechanics of Composite Materials", Hemisphere Publishing Corporation, New York, 355pp.
- Rasheed, H. A. and Yousif, O. H. (2001) "Buckling of Thin Laminated Orthotropic Rings/Long Cylinders under External Pressure," International Journal of Structural Stability and Dynamics, Vol. 1, No. 4, pp. 485-507.
- Rasheed, H. A. and Yousif, O. H. (2005) "Stability of Anisotropic Laminated Rings and Long Cylinders Subjected to External Hydrostatic Pressure," Journal of Aerospace Engineering, ASCE, Vol. 18, No. 3, pp. 129-138.
- Sparks, C. P., (1986) "Lightweight Composite Production Risers for a Deep Water Tension Leg Platform," Proceedings, 5th International OMAE Conference, Tokyo, pp. 86-93.
- Sumana, B. G., Vidya Sagar, H. N., Sharma, K. V. and Krishna, M., (2015) "Numerical analysis of the effect of fiber orientation on hydrostatic buckling behavior of fiber metal composite cylinder," Journal of Reinforced Plastics and Composites, Vol. 34 (17), pp. 1422-1432.
- Timoshenko, S. P., (1933) Applied Mechanics, ASME, APM-55-20, p. 173.